

SCIENTIFIC REPORTS

OPEN

(+)/(−)-Phaeocaulin A-D, four pairs of new enantiomeric germacrane-type sesquiterpenes from *Curcuma phaeocaulis* as natural nitric oxide inhibitors

Received: 21 October 2016

Accepted: 25 January 2017

Published: 08 March 2017

Gui-yang Xia^{1,2}, De-juan Sun², Jiang-hao Ma², Yue Liu², Feng Zhao³, Paul Owusu Donkor¹, Li-qin Ding¹, Li-xia Chen² & Feng Qiu¹

Germacrane-type sesquiterpenes, with a flexible 10-membered ring unit as the structural and conformational features, play a central role in the biosynthesis and synthesis of other sesquiterpenes. In this report, two pairs of new sesquiterpene alkaloids, (+)/(−)-phaeocaulin A [(+)-1/(−)-1] and B [(+)-2/(−)-2], and two pairs of new sesquiterpenes, (+)/(−)-phaeocaulin C [(+)-3/(−)-3] and D [(+)-4/(−)-4], along with one related known analog (5), were isolated from the rhizomes of *Curcuma phaeocaulis*. The absolute configurations of (+)-1/(−)-1, (+)-2/(−)-2, (+)-3/(−)-3 and (+)-4/(−)-4 were unambiguously determined by analysis of single-crystal X-ray diffractions and quantum chemical electronic circular dichroism (ECD) method. It is noteworthy that (+)/(−)-phaeocaulin A [(+)-1/(−)-1] and B [(+)-2/(−)-2] are two pairs of rare N-containing germacrane-type sesquiterpenes. A possible biogenetic pathway for 1–5 was postulated. All of the isolated compounds were tested for their inhibitory activity against LPS-induced nitric oxide production in RAW 264.7 macrophages.

Natural products and their derivatives have been a rich source of bioactive compounds for drug discovery and development¹. To date, more than 200 different sesquiterpene skeletons have been discovered, and these are predominantly formed from farnesyl diphosphate (FDP) as a common acyclic precursor by enzymatic cyclizations and further transformations^{2,3}. Germacrane-type sesquiterpenes, with unique structural and conformational features, are naturally occurring in plants, bacteria, fungi, and marine invertebrates. Owing to their central role in the biosynthesis of other sesquiterpenes and their potent bioactivities, germacrane-type sesquiterpenes have stimulated efforts in their isolation, synthesis and structural modification for drug discovery^{4–7}. It is not uncommon for natural products to have one or more stereogenic centers with a significant influence on biological activity^{8–10}. Different single enantiomers may have different pharmacokinetic properties (absorption, distribution, biotransformation, and excretion) and quantitatively or qualitatively different pharmacologic or toxicologic effects¹¹. The separation and configurational assignment of optically pure compounds are an important yet challenging process in structure elucidation.

Curcuma phaeocaulis Valetton, belonging to the family Zingiberaceae, is widely distributed in the southern regions of the People's Republic of China such as Sichuan, Yunnan, Guangdong, and Fujian provinces. The rhizomes of this plant, known as *Rhizoma curcumae* (*Ezhu* in Chinese), are an important crude drug frequently

¹School of Chinese Materia Medica and Tianjin State Key Laboratory of Modern Chinese Medicine, Tianjin University of Traditional Chinese Medicine, 312 Anshanxi Road, Nankai District, Tianjin 300193, People's Republic of China.

²Department of Natural Products Chemistry, School of Traditional Chinese Materia Medica, Key Laboratory of Structure-Based Drug Design & Discovery, Ministry of Education, Shenyang Pharmaceutical University, Shenyang 110016, People's Republic of China. ³School of Pharmacy, Key Laboratory of Molecular Pharmacology and Drug Evaluation (Yantai University), Ministry of Education, Collaborative Innovation Center of Advanced Drug Delivery System and Biotech Drugs in Universities of Shandong, Yantai University, Yantai, 264005, People's Republic of China. Correspondence and requests for materials should be addressed to F.Q. (email: fengqiu20070118@163.com) or L.-X.C. (email: syzylx@163.com)

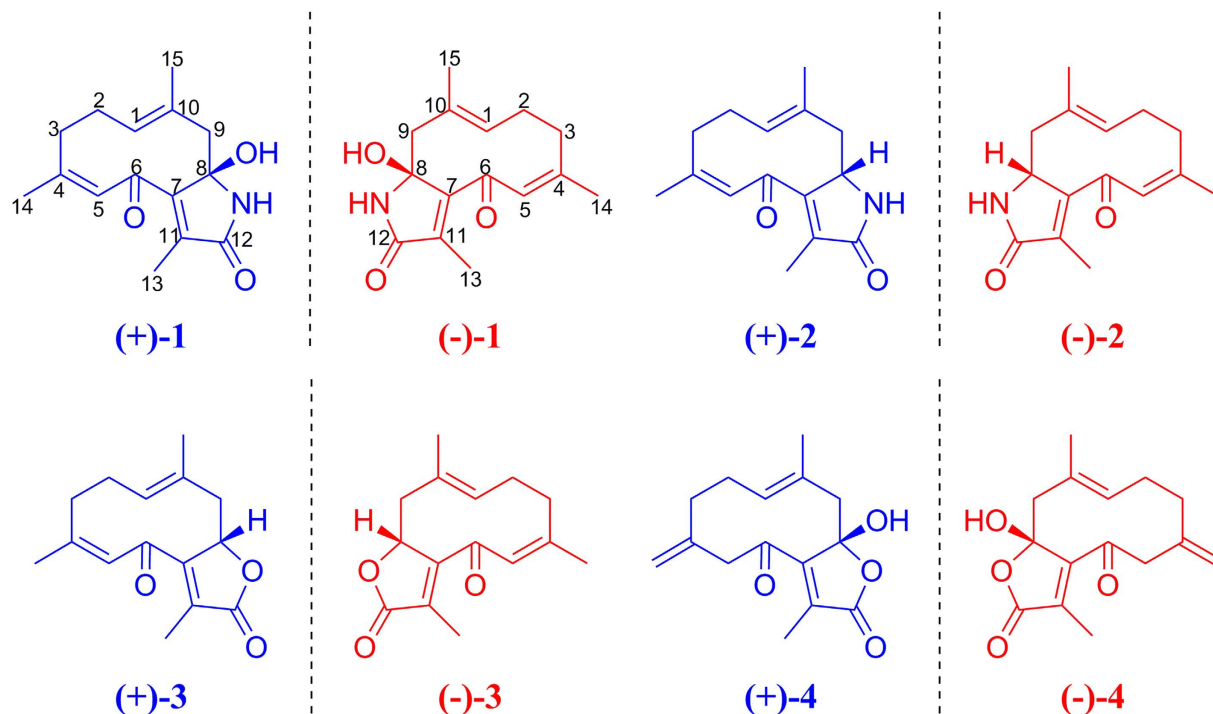


Figure 1. Chemical structures of (+)-1/(-)-1, (+)-2/(-)-2, (+)-3/(-)-3 and (+)-4/(-)-4.

listed in prescriptions of traditional Chinese medicine (TCM) for the treatment of Blood Stasis Syndrome (BSS) caused by the obstruction of blood circulation, such as arthralgia, psychataxia, and dysmenorrhea^{12,13}. Recent phytochemical investigations of this plant have revealed that its main constituents are sesquiterpenoids^{13,14}, and these constituents exhibit anti-inflammatory¹⁵, antitumor^{16,17}, and platelet aggregation inhibitory¹⁸ activities. As part of our continuing investigations into biologically active sesquiterpenoids from *C. phaeocaulis*, and to provide a potential explanation for its usage of treating inflammatory diseases in China, the remaining fractions were further fractionated to afford two rare N-containing germacrane-type sesquiterpenes, two new germacrane-type sesquiterpenes (Fig. 1), and one known germacrane derivative. Although germacrane-type sesquiterpenes are not very rare, the discovery of the unusual N atom in the skeleton of germacrane-type sesquiterpenes, coupled with the existence of enantiomers in compounds 1–5 for the single chiral center at C-8 is especially interesting. Optically pure enantiomers (+)-1/(-)-1, (+)-2/(-)-2, (+)-3/(-)-3, and (+)-4/(-)-4 were obtained with the help of chiral high-performance liquid chromatography (HPLC) separation. We describe, herein, the isolation and unequivocal characterization of these compounds, as well as their inhibitory effects on nitric oxide (NO) production in lipopolysaccharide (LPS)-activated macrophages. To our knowledge, this represents the first instance of enantiomeric separation of germacrane-type sesquiterpenes by chiral HPLC column that enables us to obtain optically pure materials for further investigations.

Results

Structure elucidation. Phaeocaulin A (1) was obtained as white needles from methanol. It was assigned the molecular formula $C_{15}H_{19}NO_3$ (seven degrees of unsaturation) on the basis of HRESIMS analysis. The IR spectrum exhibited absorptions at 3384 and 1634 cm^{-1} which were typical for the lactam group¹³. The 1H NMR spectroscopic data (Table 1) exhibited signals corresponding to three olefinic methyl groups [δ_H 1.66, 1.88 and 1.93 (each 3H, s)] and two olefinic protons [δ_H 6.37 (1H, s) and 4.92 (1H, dd, $J = 10.6, 3.6$)]. The ^{13}C NMR data (Table 1) indicated the presence of two carbonyl carbons (δ_C 172.1 and 195.3), six olefinic carbons (δ_C 128.4, 130.9, 139.4, 140.3, 148.7, and 153.7), and three methyl carbons (δ_C 10.1, 18.8, and 25.2). Extensive comparison of the 1H and ^{13}C NMR data of 1 with those of (1E,4Z)-8-hydroxy-6-oxogermacra-1(10),4,7(11)-trieno-12,8-lactone (5) which was obtained from *Chloranthus henryi*¹⁹, suggested that the structure of 1 resembled that of 5, except for the low-frequency shift of C-8. This appearance could be explained if C-8 was attached to a less electronegative atom than an oxygen atom, for instance, a nitrogen atom. This inference was confirmed by the HMBC correlations from H_3-15 to C-1/C-8/C-9/C-10, H_2-9 to C-1/C-7/C-8/C-10/C-15, and H_3-13 to C-6/C-7/C-8/C-11/C-12 (Fig. 2). It was reported that the ^{13}C NMR method could be used to predict the configuration of trisubstituted double bonds containing one methyl substituent. If the resonance for the vinylic methyl group appears at a value greater than 20 ppm, the double bond has a (Z)-configuration, whereas if the value is less than 20 ppm, an (E)-configuration is present²⁰. Therefore, the 1,10- and 4,5-double bonds were assigned as (E)- and (Z)-configurations, respectively, due to the chemical shifts of C-15 (δ_C 18.8) and C-14 (δ_C 25.2). On the basis of the above evidence, the structure of 1 was established as (1E,4Z)-8-hydroxy-6-oxogermacra-1(10),4,7(11)-trieno-12,8-lactam.

Position	1 ^a		2 ^a		3 ^b		4 ^b	
	¹ H	¹³ C ^c	¹ H	¹³ C ^c	¹ H	¹³ C ^d	¹ H	¹³ C ^d
1	4.92 (dd, 10.6, 3.6)	128.4	4.90 (m)	129.2	5.01 (brs)	128.7	5.27 (d, 7.9)	130.7
2	2.06 (m)	26.9	2.16 (m)	28.4	2.16 (m)	27.0	2.14 (m)	29.3
	2.20 (ddd, 24.0, 12.0, 3.3)		2.16 (m)		2.16 (m)		2.22 (m)	
3	2.89 (m)	31.0	3.00 (m)	32.6	3.01 (m)	30.8	2.40 (m)	36.2
	2.11 (m)		2.10 (m)		2.14 (m)		2.12 (m)	
4		148.7		151.4		150.6		140.3
5	6.37 (s)	130.9	6.30 (s)	130.6	6.17 (brs)	127.7	3.45 (s)	50.7
6		195.3		196.0		191.1		197.1
7		153.7		156.3		158.1		154.7
8		92.8	4.64 (d, 9.8)	60.4	5.24 (brs)	80.1		110.4
9	2.24 (d, 12.8)	50.3	2.63 (dd, 11.8, 3.1)	47.3	2.86 (dd, 11.8, 3.7)	45.5	2.32 (d, 13.3)	49.9
	2.69 (d, 12.8)		1.96 (m)		2.18 (m)		2.86 (d, 13.3)	
10		139.4		138.1		133.6		135.4
11		140.3		140.9		132.9		130.5
12		172.1		175.1		172.9		170.4
13	1.93 (s)	10.1	1.91 (s)	10.8	2.03 (s)	9.9	2.00 (s)	10.6
14	1.88 (s)	25.2	1.92 (s)	25.9	1.93 (s)	25.0	4.95 (s)	119.2
							5.12 (s)	
15	1.66 (s)	18.8	1.61 (s)	17.7	1.60 (s)	16.6	1.64 (s)	17.8

Table 1. ¹H NMR (600 MHz) and ¹³C NMR data for compounds 1–4 (δ in ppm, J in Hz). ^aSpectra were obtained in CD₃OD. ^bSpectra were obtained in CDCl₃. ^cRecorded at 75 MHz. ^dRecorded at 150 MHz.

Phaeocaulin B (**2**) was obtained as white needles from methanol and has the molecular formula C₁₅H₁₉NO₂ with seven degrees of unsaturation, as deduced from the HRESIMS analysis (m/z 268.1307 [M+Na]⁺, calcd for 268.1308). The structure of **2** was mainly determined by comparing its NMR spectroscopic data (Table 1) with those of **1**. The absence of the hydroxy group at C-8 in **2** was suggested by the molecular formula (C₁₅H₁₉NO₂) and the up-field shift of C-8 (δ_C 60.4 in **2** and δ_C 92.8 in **1**), as well as the presence of the hydrogen signal at δ_H 4.64. This deduction was supported by the HMBC correlations from H-9a to C-8, and H₃-15 to C-1/C-7/C-8/C-9/C-10. Thus, the structure of compound **2** was established as (1E,4Z)-6-oxogermacra-1(10),4,7(11)-trieno-12,8-lactam.

Phaeocaulin C (**3**) was obtained as colorless cube crystals from methanol and yielded a quasi-molecular ion peak in the HRESIMS spectrum at m/z 247.1336 [M+H]⁺, which indicated a molecular formula of C₁₅H₁₈O₃ in conjunction with ¹³C NMR data. A single-crystal X-ray diffraction analysis of **3** (See Supplementary data) showed that the main skeleton of **3** was a germacrane-type sesquiterpene. The IR spectrum revealed the presence of an α,β -unsaturated γ -lactone (1762 cm⁻¹) group. In the ¹H NMR spectrum of **3** (Table 1), the characteristic protons for two olefinic protons [δ_H 5.01 (1H, brs) and 6.17 (1H, s)] and three methyl groups [δ_H 1.60 (3H, s), 1.93 (3H, s), and 2.03 (3H, s)] were observed. The ¹³C NMR spectroscopic data of **3** (Table 1) showed the presence of 15 carbon atoms, including three methyls, three methylenes, three methines and six quaternary carbons. Comparing the ¹H and ¹³C NMR spectra of **3** with those of **5**, the hemiketal carbon present in **5**¹⁹ was missing and an additional oxymethine was observed at δ_H 5.24 (1H, brs) and δ_C 80.1. According to the aforementioned information, the structure of **3** was assigned as an 8-deoxy derivative of **5**. This deduction was supported by the HMBC correlations from H-9a to C-1/C-7/C-8/C-10/C-15. Thus, the structure of compound **3** was assigned as (1E,4Z)-6-oxogermacra-1(10),4,7(11)-trieno-12,8-lactone.

Phaeocaulin D (**4**) was assigned the molecular formula C₁₅H₁₈O₄ according to a quasi-molecular ion at m/z 285.1096 [M+Na]⁺ in its HRESIMS spectrum. The ¹H NMR spectrum showed signals corresponding to two methyl groups δ_H 1.64 (3H, s) and 2.00 (3H, s). The ¹³C NMR spectroscopic data (Table 1) indicated the presence of two carbonyl carbons (δ_C 197.1 and 170.4), one hemiketal carbon (δ_C 110.4), six olefinic carbons (δ_C 119.2, 130.5, 130.7, 135.4, 140.3 and 154.7), and two methyl carbons (δ_C 10.6 and 17.8). The ¹H and ¹³C NMR spectra of **4** were similar to those of **5**¹⁹, except for the absence of one methyl group and the appearance of one 1,1-disubstituted double bond. Its position could be determined by the key HMBC correlations from H-14a to C-3/C-4/C-5/C-6, H-14b to C-2/C-3/C-4/C-5/C-6, and H₂-5 to C-3/C-4/C-6/C-14. The substituted positions of the CH₃-13 and CH₃-15 were determined by the HMBC correlations from H₃-13 to C-7/C-11/C-12 and H₃-15 to C-1/C-9/C-10. The 1,10-double bond was assigned an (*E*)-configuration due to the chemical shift of C-15 (δ_C 17.8)²⁰. On the basis of all the above evidences, the structure of **4** was elucidated as (1E)-8-hydroxy-6-oxogermacra-1(10),4(14),7(11)-trieno-12,8-lactone.

Stereochemical issues. Although compounds **1–5** all possess a chiral carbon at C-8, the specific optical rotations were, in all cases, close to zero. Moreover, no Cotton effects (CEs) were observed in their ECD spectra. It suggested that these chiral compounds might be obtained as racemic mixtures. This speculation was confirmed by the X-ray analysis of **1–3** and **5** which crystallized in space groups containing inversion centers or glide planes²¹.

Compounds **1–5** were further subjected to HPLC separation on chiral columns (Chiralpak IE and Chiralpak AD-RH). The chiral HPLC analysis of each of **1–4** showed well-resolved peaks of two enantiomers on the

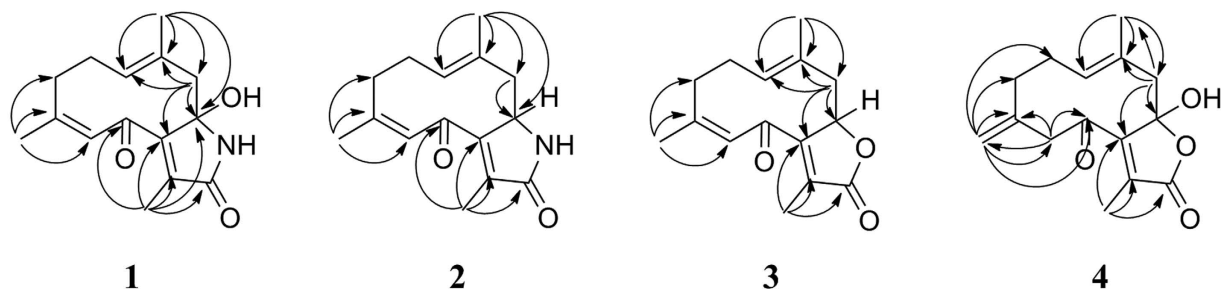


Figure 2. Key HMBC correlations of compounds 1, 2, 3 and 4.

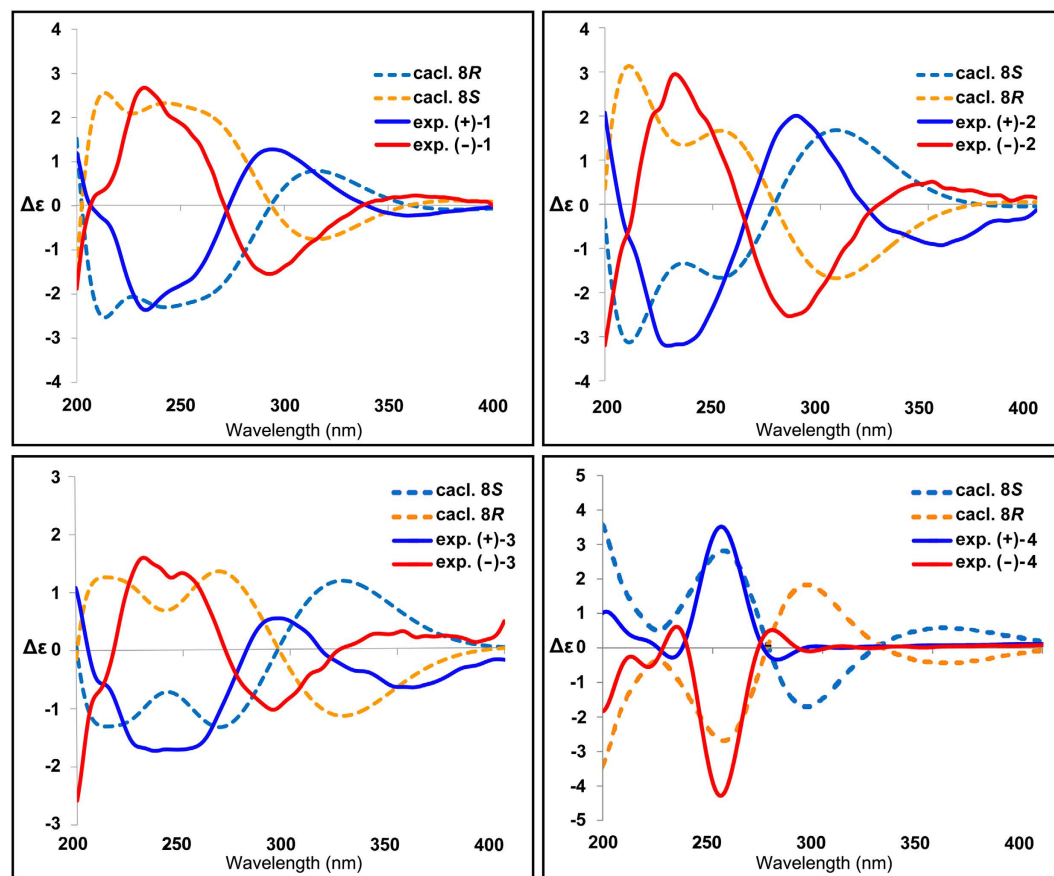


Figure 3. Experimental ECD spectra of compounds (+)-1/(-)-1, (+)-2/(-)-2, (+)-3/(-)-3 and (+)-4/(-)-4 and calculated ECD spectra of 8S/8R of 1-4.

Chiralpak IE column (250 mm × 4.6 mm, 5 μm; Daicel) with *n*-hexane/isopropanol at a rate of 0.8 mL min⁻¹. The relative abundance of each pair was ca. 1:1 according to their relative peak areas in the HPLC chromatograms. Efforts were made to get the enantiomers of 5 separated. Unfortunately, no well-resolved peaks were observed with changing columns and methods. Finally, chiral semi-preparative HPLC purifications were undertaken for compounds 1-4, yielding (+)-1/(-)-1, (+)-2/(-)-2, (+)-3/(-)-3, and (+)-4/(-)-4. Each of these compounds showed typical antipodal ECD curves (Fig. 3) and specific rotations of opposite sign.

Pure enantiomers of (-)-1 (CCDC 1486406), (+)-3 (CCDC 1486411), and (-)-3 (CCDC 1486410) were further recrystallized in methanol to obtain single crystals for X-ray structure determination using Cu Kα radiation (Fig. 4) which allowed for the determination of the absolute configuration of C-8 in (-)-1 and (+)-3 as 8S and that of their enantiomers (+)-1 and (-)-3 as 8R.

Computational calculations of ECD²²⁻²⁴ spectra of the 8S/8R enantiomers of compounds 1-4 were performed. Comparison of these calculated spectra with the experimental ECD spectra obtained from the isolated enantiomers allowed us to determine their absolute configurations (Fig. 3). Consequently, the absolute configurations of C-8 in (+)-1/(-)-1, (+)-2/(-)-2, (+)-3/(-)-3 and (+)-4/(-)-4 were unambiguously determined.

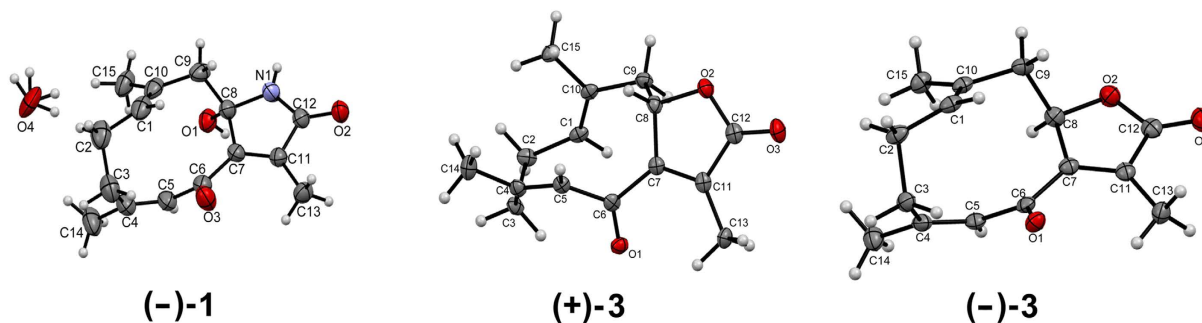


Figure 4. ORTEP drawings of compounds (-)-1, (+)-3, and (-)-3.

Compounds	IC ₅₀ ± SD (μM)	Compounds	IC ₅₀ ± SD (μM)
(±)-1	57.63 ± 4.44	(±)-3	28.72 ± 2.80
(+)-1	35.97 ± 3.13	(+)-3	20.43 ± 2.26
(-)-1	57.25 ± 4.27	(-)-3	23.85 ± 2.20
(±)-2	44.18 ± 3.91	(±)-4	29.17 ± 2.78
(+)-2	24.02 ± 1.99	(±)-5	17.34 ± 1.65
(-)-2	47.95 ± 3.68	Hydrocortisone	48.66 ± 3.26

Table 2. NO inhibitory activity of compounds 1–5.

	(+)-1	(-)-1	(+)-2	(-)-2	(+)-3	(-)-3	(+)-4	(-)-4
C-8	R	S	S	R	S	R	S	R
Retention time (min) ^a	7.0	15.4	9.7	10.9	10.8	12.2	9.7	11.1
Optical rotation [α] _D ²⁵	+25.7	-32.9	+43.1	-32.0	+68.0	-46.3	+106.7	-88.9
CEs	200–205 nm	+	-	+	-	+	-	+
	220–260 nm	-	+	-	+	-	+	-
	280–310 nm	+	-	+	-	+	-	+

Table 3. Characteristic features for the enantiomers. ^aFor chromatographic conditions, see extraction and isolation section.

Inhibitory effect of the isolated compounds on NO production induced by LPS in macrophages. Nitric oxide produced by a group of nitric oxide synthases (NOSs) is highly diffusible across cell membranes and modifies many biological molecules. It plays an important role in the inflammatory process, and an inhibitor of NO production may be considered as a potential anti-inflammatory agent^{25,26}. To confirm the bioactive secondary metabolites responsible for the anti-inflammatory activity of *C. phaeocaulis*, all isolated compounds were tested for their inhibitory effects on NO production induced by LPS in macrophages (pure enantiomers of **4** were not measured due to paucity of the sample) (Table 2). In comparison with the positive control, hydrocortisone (IC₅₀ 48.66 μM), most of the compounds exhibited moderate inhibitory activities against NO production with IC₅₀ values in the range of 17.34 to 30.02 μM. The possible mechanisms of these active compounds remain to be further explored.

Discussion

The characteristic features for each pair of enantiomers were summarized in Table 3. The empirical CD rules have been successfully employed in determining the stereochemistry of the α,β-unsaturated lactone or lactam rings in various natural products^{27–29}. However, it seems that the rules are not entirely applicable to these four pairs of germacrane-type sesquiterpenes, which could be attributed to the neighboring high conformational flexible ten-membered ring and the presence of the polyunsaturated conjugated chromophores around the stereogenic center (C-8)^{28,29}. This was confirmed by the shifts of CEs at ca. 220 and 250 nm in the CD spectra of (-)-**4**/(+)-**4** when compared to (-)-**1**/(+)-**1**, (-)-**2**/(+)-**2**, and (-)-**3**/(+)-**3**. Here, characteristic ECD spectra of four pairs of unambiguously determined germacrane-type sesquiterpene enantiomers were provided. Further study is also required to elucidate the underlying mechanism behind the observation of the CEs.

The germacrane-type sesquiterpenes with a flexible 10-membered ring system, are biogenetically generated from FDP and play a central role in the biosynthesis or synthesis of other sesquiterpenes. The discovery of sesquiterpene alkaloids (+)-**1**/(-)-**1** and (+)-**2**/(-)-**2** in *Curcuma* genus is rather unusual from a chemotaxonomic perspective. These type of alkaloids are synthesized primarily from non-amino acid precursors, with the nitrogen

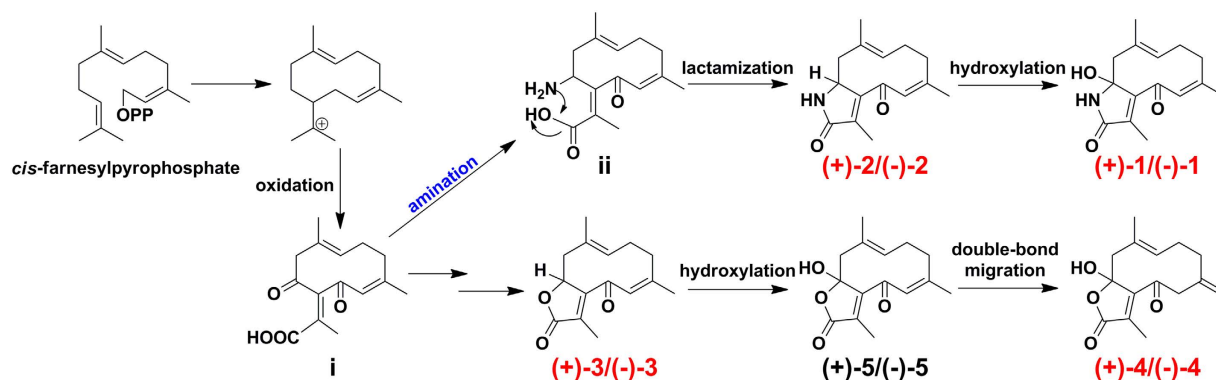


Figure 5. Plausible biogenetic pathway of 1–5.

atom being inserted into the structure at a relatively late stage by amination processes³⁰. The proposed biosynthesis of 1–5 was shown in Fig. 5. First, the 10-membered ring systems could be formed by a cyclization of the *cis*-farnesylpyrophosphate. Following a series of enzymatic oxidations, the intermediate **i** could be generated. Then, the important intermediate **ii** could be derived from **i** via amination reactions. The racemization of 1–5 could be explained by the intramolecular lactamization or lactonization, which might be non-stereoselective. Under enzyme catalysis, (+)-2/(-)-2 and (+)-3/(-)-3 could then undergo hydroxylation to yield the racemates (+)-1/(-)-1 and (+)-5/(-)-5, respectively. Ultimately, the racemates (+)-4/(-)-4 could be generated from (+)-5/(-)-5 via the migration of the double bonds.

Conclusion

The current study reported the isolation and structure elucidation of two rare germacran-type sesquiterpene alkaloids (**1** and **2**) and two new germacran-type sesquiterpenes (**3** and **4**) from the rhizomes of *Curcuma phaeocaulis*. The chiral resolution of the enantiomeric germacran-type sesquiterpenes, (+)-1/(-)-1, (+)-2/(-)-2, (+)-3/(-)-3, and (+)-4/(-)-4, permitted the unambiguous definition of the absolute configurations of the optically pure enantiomers via X-ray diffraction analysis and computation of ECD spectra, which provides powerful models for the absolute configuration studies of this class of compounds. Inhibitory effects of the isolated compounds on nitric oxide production in LPS-activated macrophages were evaluated. Most of the isolated compounds exhibited more potent inhibition than the positive control, hydrocortisone, indicating their potential as promising compounds for further research and development of anti-inflammatory agents. The whole spectroscopic data, including the computation of ECD spectra, will provide additional evidence for the absolute configuration of similar structures.

Methods

General. The melting point (uncorrected) was determined on an X-4 digital display micromelting point apparatus. Optical rotations were measured with a Perkin-Elmer 241 polarimeter. UV spectra were recorded on a Shimadzu UV 2201 spectrophotometer. IR spectra were recorded on a Bruker IFS 55 spectrometer. CD spectra were recorded on a Bio-Logic Science MOS-450 spectrometer. NMR experiments were performed on Bruker ARX-300 and AV-600 spectrometers. HRESIMS were obtained on an Agilent 6210 TOF mass spectrometer. Silica gel GF254 prepared for TLC and silica gel (200–300 mesh) for column chromatography were obtained from Qingdao Marine Chemical Factory (Qingdao, People's Republic of China). Octadecyl silica gel was purchased from Merck Chemical Company Ltd. RP-HPLC separations were conducted using an LC-6AD liquid chromatograph with a YMC Pack ODS-A column (250 × 20 mm, 5 μm, 120 Å) and an SPD-10A VP UV/VIS detector. Analysis and chiral purifications of racemates of 1–4 were carried out on a Chiralpak IE column (150 mm × 4.6 mm, 5 μm; Daicel Chemical Industries, Ltd). All reagents were of HPLC or analytical grade and were purchased from Tianjin Damao Chemical Company. Spots were detected on TLC plates under UV light or by heating after spraying with anisaldehyde-H₂SO₄.

Plant material. Rhizomes of *C. phaeocaulis* were collected from Chengdu, Sichuan Province, China, and identified by Professor Qishi Sun, Department of Pharmaceutical Botany, School of Traditional Chinese Materia Medica, Shenyang Pharmaceutical University. A voucher specimen (CP-20100715) has been deposited in the herbarium of the Department of Natural Products Chemistry, Shenyang Pharmaceutical University.

Extraction and isolation. Dry rhizomes of *C. phaeocaulis* (10 kg) were cut into approximately 2 cm pieces and extracted with 95% aqueous EtOH (2 × 100L × 2 h). After evaporation of the combined EtOH extracts *in vacuo*, the resulting concentrated extract (0.6 kg) was suspended in H₂O (3L), and partitioned successively with cyclohexane, EtOAc, and *n*-BuOH (3 × 3L). The cyclohexane extract (170 g) was subjected to silica gel column (10 × 80 cm) eluted with hexane/EtOAc (100:1, 40:1, 20:1, 10:1, 4:1, 2:1, 1:1, and 0:1 v/v) to obtain fractions CA–CH. Fraction CA (5 g) was subjected to silica gel column (3 × 40 cm) eluted with petroleum ether/acetone (from 40:1 to 0:1) to produce seven fractions (CA1–CA7). Fraction CB (20 g) was subjected to silica gel column

(6 × 80 cm) eluted with cyclohexane/acetone (from 40:1 to 0:1) to produce five fractions (CB1–CB5). Fraction CB1 (2 g) was chromatographed over a silica gel column (3 × 40 cm) eluted with petroleum ether/acetone (from 40:1 to 0:1) to produce fractions CB11–CB13. Fraction CB11 (20.0 mg) was recrystallized to give compound **1** (22.6 mg), while (+)-**1** (3.9 mg, $t_R = 7.0$ min) and (–)-**1** (3.8 mg, $t_R = 15.4$ min) were obtained from a chiral column (Chiralpak IE) under normal phase conditions (*n*-hexane:isopropanol = 1:1) at 0.8 mL/min using a UV detector at 220 nm. Fraction CB4 (3.5 g) was subjected to reversed-phase C_{18} silica gel column (2.5 × 30 cm) eluted with MeOH/H₂O (1:9 to 8:2) to yield CB41, CB42 and CB43. CB42 (80 mg) was separated by HPLC (60% MeOH/H₂O) to afford compound **2** (10.5 mg, $t_R = 45$ min), while (+)-**2** (2.7 mg, $t_R = 9.7$ min) and (–)-**2** (2.5 mg, $t_R = 10.9$ min) were obtained from a chiral column (Chiralpak IE) under normal phase conditions (*n*-hexane:isopropanol = 1:1) at 0.8 mL/min using a UV detector at 220 nm. Fraction CC (19 g) was subjected to silica gel column (6 × 80 cm) chromatography eluting with petroleum ether/EtOAc (from 40:1 to 0:1) to produce seven fractions (CC1–CC7). Fraction CC1 (25 mg) was recrystallized to give compound **5** (14.2 mg). Fraction CD (6.2 g) was chromatographed using reversed-phase C_{18} silica gel column (2.5 × 30 cm) eluting with MeOH/H₂O (30:70, 50:50, 70:30 and 100:0, v/v) to give three fractions CD1–CD3, and subfraction CD1 (54 mg) was separated by preparative HPLC (50% MeOH/H₂O, 6 mL/min) to afford compound **4** (2.5 mg, $t_R = 60$ min), while (+)-**4** (0.6 mg, $t_R = 9.7$ min) and (–)-**4** (0.6 mg, $t_R = 11.1$ min) were obtained from a chiral column (Chiralpak IE) under normal phase conditions (*n*-hexane:isopropanol = 4:1) at 0.8 mL/min using a UV detector at 220 nm. The EtOAc extract (105 g) was subjected to silica gel column (10 × 80 cm) eluted with cyclohexane/acetone (100:1, 40:1, 20:1, 10:1, 4:1, 2:1, 1:1, and 0:1 v/v) to obtain five fractions (EA–EF). Fraction EC (15 g) was subjected to silica gel column (6 × 80 cm) eluted with a gradient of increasing acetone (0–100%) in *n*-hexane to afford fractions EC1–EC7. EC3 (4.8 g) was chromatographed over a reversed-phase C_{18} silica gel column (2.5 × 30 cm) eluted with MeOH/H₂O (30:70, 50:50, 70:30 and 100:0 v/v) to give four fractions EC3-1 to EC3-4, and subfraction EC3-3 (160 mg) was separated by preparative HPLC (40% MeOH/H₂O, 6.0 mL/min) to afford compound **3** (33.2 mg, $t_R = 73$ min), while (+)-**3** (4.3 mg, $t_R = 10.8$ min) and (–)-**3** (4.2 mg, $t_R = 12.2$ min) were obtained from a chiral column (Chiralpak IE) under normal phase conditions (*n*-hexane:isopropanol = 1:1) at 0.8 mL/min using a UV detector at 220 nm.

Spectroscopic data of the isolated compounds. **Phaeocaulin A (1):** white needles; $[\alpha]_D^{25} -4.5$ (c 0.1, MeOH); UV (MeOH) λ_{max} (log ϵ) 233 (4.14) nm; IR (KBr) ν_{max} : 3384, 2945, 2833, 1634, 1450, 1384, 1118, 1030 cm^{-1} ; HR-ESI-MS m/z 284.1257 $[M+Na]^+$ (calcd for $C_{15}H_{19}NO_3Na$, 284.1263); ¹H and ¹³C NMR data, see Table 1.

(+)-**Phaeocaulin A** [(+)-**1**]: white powder; $[\alpha]_D^{25} +25.7$ (c 0.05, MeOH); CD (CH₃OH, 1.9 mM) λ_{max} ($\Delta\epsilon$) 233 (–5.70), 294 (+3.03), 360 (–0.56).

(–)-**Phaeocaulin A** [(–)-**1**]: colorless needles; m.p. 179.0–180.0 °C; $[\alpha]_D^{25} -32.9$ (c 0.05, MeOH); CD (CH₃OH, 1.5 mM) λ_{max} ($\Delta\epsilon$) 233 (+2.66), 293 (–1.56), 363 (+0.22).

Phaeocaulin B (2): white needles; $[\alpha]_D^{25} +5.0$ (c 0.1, MeOH); UV (MeOH) λ_{max} (log ϵ) 242 (3.90) nm; IR (KBr) ν_{max} : 3407, 2936, 2833, 1692, 1660, 1631, 1448, 1384, 1118, 1030 cm^{-1} ; HR-ESI-MS m/z 268.1307 $[M+Na]^+$ (calcd for $C_{15}H_{19}NO_2Na$, 268.1308); ¹H and ¹³C NMR data, see Table 1.

(+)-**Phaeocaulin B** [(+)-**2**]: white powder; $[\alpha]_D^{25} +43.1$ (c 0.05, MeOH); CD (CH₃OH, 0.4 mM) λ_{max} ($\Delta\epsilon$) 229 (–3.21), 288 (+2.01), 356 (–0.93).

(–)-**Phaeocaulin B** [(–)-**2**]: white powder; $[\alpha]_D^{25} -32.0$ (c 0.05, MeOH); CD (CH₃OH, 0.4 mM) λ_{max} ($\Delta\epsilon$) 233 (+2.95), 286 (–2.54), 352 (+0.51).

Phaeocaulin C (3): colorless cube crystals; $[\alpha]_D^{25} -2.4$ (c 0.07, MeOH); UV (MeOH) λ_{max} (log ϵ) 228 (4.02) nm; IR (KBr) ν_{max} : 2930, 2855, 1762, 1667, 1644, 1622, 1444, 1384, 1154, 1015 cm^{-1} ; HRESIMS (positive) m/z : 247.1336 $[M+H]^+$ (calcd for $C_{15}H_{19}O_3$, 247.1334); ¹H and ¹³C NMR data, see Table 1.

(+)-**Phaeocaulin C** [(+)-**3**]: colorless needles; m.p. 108.0–109.0 °C; $[\alpha]_D^{25} +68.0$ (c 0.04, MeOH); CD (CH₃OH, 0.4 mM) λ_{max} ($\Delta\epsilon$) 237 (–1.74), 295 (+0.53), 357 (–0.67).

(–)-**Phaeocaulin C** [(–)-**3**]: colorless needles; m.p. 108.0–109.0 °C; $[\alpha]_D^{25} -46.3$ (c 0.04, MeOH); CD (CH₃OH, 0.4 mM) λ_{max} ($\Delta\epsilon$) 232 (+1.59), 292 (–1.04), 353 (+0.29).

Phaeocaulin D (4): yellowish oil; $[\alpha]_D^{25} +6.0$ (c 0.1, MeOH); UV (MeOH) λ_{max} (log ϵ) 213 (1.63) nm; IR (KBr) ν_{max} : 3398, 2943, 2833, 1764, 1642, 1449, 1384, 1127, 1030 cm^{-1} ; HRESIMS (positive) m/z : 285.1096 $[M+Na]^+$ (calcd for $C_{15}H_{18}O_4Na$, 285.1097); ¹H and ¹³C NMR data, see Table 1.

(+)-**Phaeocaulin D** [(+)-**4**]: yellowish oil; $[\alpha]_D^{25} +106.7$ (c 0.015, MeOH); CD (CH₃OH, 0.6 mM) λ_{max} 254 (+1.86).

(–)-**Phaeocaulin D** [(–)-**4**]: yellowish oil; $[\alpha]_D^{25} -88.9$ (c 0.02, MeOH); CD (CH₃OH, 0.8 mM) λ_{max} 254 (–1.70).

Single-Crystal X-ray Diffraction Analysis and Crystallographic Data of Compounds **1**, (–)-**1**, **2**, **3**, (+)-**3**, (–)-**3**, and **5**, NO production bioassay, see Supplementary information.

References

- Eder, J., Sedrani, R. & Wiesmann, C. The discovery of first-in-class drugs: origins and evolution. *Nat Rev Drug Discov* **13**, 577–587 (2014).
- Bülow, N. & König, W. A. The role of germacrene D as a precursor in sesquiterpene biosynthesis: investigations of acid catalyzed, photochemically and thermally induced rearrangements. *Phytochemistry* **55**, 141–168 (2000).
- Cane, D. E. Enzymic formation of sesquiterpenes. *Chem Rev* **90**, 1089–1103 (1990).
- Yang, Z. J. *et al.* Syntheses and Biological Evaluation of Costunolide, Parthenolide, and Their Fluorinated Analogues. *J Med Chem* **58**, 7007–7020 (2015).
- Long, J. *et al.* Total Syntheses of Parthenolide and Its Analogues with Macrocyclic Stereocontrol. *J Med Chem* **57**, 7098–7112 (2014).
- Fraga, B. M. Natural sesquiterpenoids. *Nat Prod Rep* **30**, 1226 (2013).

7. Minnaard, A. J., Wijnberg, J. B. P. A. & de Groot, A. The synthesis of germacrane sesquiterpenes and related compounds. *Tetrahedron* **55**, 2115–2146 (1999).
8. Hu, Y. *et al.* (±)-Homocrepidine A, a Pair of Anti-inflammatory Enantiomeric Octahydroindolizine Alkaloid Dimers from *Dendrobium crepidatum*. *J Nat Prod* **79**, 252–256 (2016).
9. Zhao, S. M. *et al.* New cytotoxic naphthohydroquinone dimers from *Rubia alata*. *Org Lett* **16**, 5576–5579 (2014).
10. Clemons, P. A. *et al.* Small molecules of different origins have distinct distributions of structural complexity that correlate with protein-binding profiles. *Proc Natl Acad Sci USA* **107**, 18787–18792 (2010).
11. US Food Drug Administration, FDA's policy statement for the development of new stereoisomeric drugs. *Chirality* **4**, 338–340 (1992).
12. Liu, Y. *et al.* Guaiane-type sesquiterpenes from *Curcuma phaeocaulis* and their inhibitory effects on nitric oxide production. *J Nat Prod* **76**, 1150–1156 (2013).
13. Ma, J. H. *et al.* Natural nitric oxide (NO) inhibitors from the rhizomes of *Curcuma phaeocaulis*. *Org Biomol Chem* **13**, 8349–8358 (2015).
14. Yang, F. Q. *et al.* Identification and quantitation of eleven sesquiterpenes in three species of *Curcuma* rhizomes by pressurized liquid extraction and gas chromatography-mass spectrometry. *J Pharm Biomed Anal* **39**, 552–558 (2005).
15. Tohda, C., Nakayama, N., Hatanaka, F. & Komatsu, K. Comparison of Anti-inflammatory Activities of Six *Curcuma* Rhizomes: A Possible Curcuminoid-independent Pathway Mediated by *Curcuma phaeocaulis* Extract. *Evid Based Compl Alt Med* **3**, 255–260 (2006).
16. Qin, B. *et al.* “Mirror-image” manipulation of curdione stereoisomer scaffolds by chemical and biological approaches: development of a sesquiterpenoid library. *J Nat Prod* **78**, 272–278 (2015).
17. Chen, X. *et al.* Anti-tumor potential of ethanol extract of *Curcuma phaeocaulis* Valetton against breast cancer cells. *Phytomedicine* **18**, 1238–1243 (2011).
18. Mao, C., Xie, H. & Lu, T. Studies on antiplatelet aggregation and analgesic action of *Curcuma phaeocaulis*. *J Chin Med Mater* **23**, 212–213 (2000).
19. Wu, B., He, S., Wu, X. D. & Pan, Y. J. New tyrosinase inhibitory sesquiterpenes from *Chloranthus henryi*. *Chem Biodivers* **5**, 1298–1303 (2008).
20. Lange, G. L. & Lee, M. ¹³C NMR determination of the configuration of methyl-substituted double bonds in medium- and large-ring terpenoids. *Magn Reson Chem* **24**, 656–658 (1986).
21. Glusker, J. P., Lewis, M. & Rossi, M. *Crystal Structure Analysis for Chemistry and Biologists*. Vol. 16 (John Wiley & Sons, 1994).
22. Zhang, S., Hu, D.-B., He, J.-B., Guan, K.-Y. & Zhu, H.-J. A novel tetrahydroquinoline acid and a new racemic benzofuranone from *Capparis spinosa* L., a case study of absolute configuration determination using quantum methods. *Tetrahedron* **70**, 869–873 (2014).
23. Yu, H. *et al.* Pestalotiopsis C, stereochemistry of a new caryophyllene from a fungus of *Trichoderma* sp. and its tautomerization characteristics in solution. *Tetrahedron* **71**, 3491–3494 (2015).
24. Zhu, H.-J. *Organic Stereochemistry: Experimental and Computational Methods*. (Wiley-VCH, 2015).
25. Laskin, D. L. & Pendino, K. J. Macrophages and inflammatory mediators in tissue injury. *Annu Rev Pharmacol* **35**, 655–677 (1995).
26. Kroncke, Fehsel & Kolb, B. Inducible nitric oxide synthase in human diseases. *Clin Exp Immunol* **113**, 147–156 (1998).
27. Uchida, I. & Kuriyama, K. The π - π circular dichroism of $\delta\beta$ -unsaturated γ -lactones. *Tetrahedron Lett* **15**, 3761–3764 (1974).
28. Gawronski, J. K., van Oeveren, A., van der Deen, H., Leung, C. W. & Feringa, B. L. Simple Circular Dichroic Method for the Determination of Absolute Configuration of 5-Substituted 2(5H)-Furanones. *J Org Chem* **61**, 1513–1515 (1996).
29. Cuiper, A. D. *et al.* Determination of the Absolute Configuration of 3-Pyrrolin-2-ones. *J Org Chem* **64**, 2567–2570 (1999).
30. Dewick, P. M. *Medicinal Natural Products A Biosynthetic Approach 3rd Edition*. (John Wiley & Sons, Ltd., 2009).

Acknowledgements

This work was financially supported by grants from the National Natural Science Foundation of China (NSFC) (Grant No. 81430095). We are grateful to Prof. Hao Gao (Jinan University, Guangzhou, China) and Prof. Huajie Zhu (Hebei University, Baoding, China) for the X-ray diffraction analysis and the ECD calculations.

Author Contributions

F.Q. and L.-X.C. initiated the project. F.Q., L.-X.C., and G.-Y.X. designed and coordinated the project. G.-Y.X., D.-J.S., J.-H.M., and Y. L. performed the extraction, isolation, and structural identification of the compounds. F.Z. carried out the NO production bioassay. L.-Q.D. analyzed the data of the biological assay. The manuscript was prepared by G.-Y.X. and P.O.D. All authors approved the final version of the manuscript.

Additional Information

Supplementary information accompanies this paper at <http://www.nature.com/srep>

Competing financial interests: The authors declare no competing financial interests.

How to cite this article: Xia, G.- *et al.* (+)/(-)-Phaeocaulin A-D, four pairs of new enantiomeric germacrane-type sesquiterpenes from *Curcuma phaeocaulis* as natural nitric oxide inhibitors. *Sci. Rep.* **7**, 43576; doi: 10.1038/srep43576 (2017).

Publisher's note: Springer Nature remains neutral with regard to jurisdictional claims in published maps and institutional affiliations.



This work is licensed under a Creative Commons Attribution 4.0 International License. The images or other third party material in this article are included in the article's Creative Commons license, unless indicated otherwise in the credit line; if the material is not included under the Creative Commons license, users will need to obtain permission from the license holder to reproduce the material. To view a copy of this license, visit <http://creativecommons.org/licenses/by/4.0/>

© The Author(s) 2017